Publ. Astron. Soc. Aust., 1999, 16, 134–8

Two New Planetary Nebulae and an AGN in the Galactic Plane

S. H. Beer and A. E. Vaughan

School of Mathematics, Physics, Computing and Electronics,
Macquarie University, North Ryde, NSW 2109, Australia

Received 1998 September 28, accepted 1999 April 13

Abstract: A search for planetary nebulae was carried out using candidates selected by their infrared colours and 5 GHz radio emission. One new planetary nebula was identified on the basis of its small angular size, strong [O III] emission and infrared colours. Another object, known as the possible planetary nebula Wray 16–28, is similarly identified as a planetary nebula. An undiscovered AGN was also found, and is classed as a Seyfert 2 galaxy on the basis of its strong O III emission, linewidths of ∼500 km s^{-1}, and 5 GHz radio flux. Low-resolution optical spectra are presented and distance estimates discussed.

Keywords: planetary nebulae: general — galaxies: active — galaxies: Seyfert

1 Introduction

A method of detecting new planetary nebulae (PN) based on their infrared colours from the IRAS Point Source Catalogue is described by Pottasch et al. (1988). This method has been used in several subsequent investigations, for example those by Van de Steene & Pottasch (1993) and Van de Steene, Sahu & Pottasch (1996). The method is based on the fact that the vast majority of PN fall within the colour box bounded by F12/F25 $\leq 0{\cdot}35$ and F25/F60 $\geq 0{\cdot}35$, where F12, F25, and F60 refer to the fluxes in the IRAS wavelength bands centred at 12, 25 and 60 μm respectively.

In this investigation, sources were chosen from inside this colour box that were also present in the Parkes–MIT–NRAO (PMN) 5 GHz Catalogue of Point Sources. A list of 206 sources was compiled in this way, and it was found that 115 corresponded to known PN. A shortlist of 75 candidate fields was compiled, containing no known PN and no obvious correspondence with other known objects (typically H II regions, SNR).

2 Observations

Observations were carried out in 53 of the candidate fields in 1998 January on the 74 in Telescope at Mount Stromlo Observatory. The Boller & Chivens Cassegrain Spectrograph was used, with the 300 line/mm grating blazed at 5000 Å. Approximate flux calibration was made using observations of a single source, HR 3454, as precise flux measurements were not needed. Finder charts were constructed from Digitized Sky Survey (DSS) images obtained from the SkyView Virtual Observatory. It was necessary to take spectra of several objects in each field, most of which turned out to be ordinary stars.

Spectra were taken of 112 objects from 3800 to 5300 Å. The spectra were reduced using IRAF, and nine objects with PN-like emission-line spectra were found. However, six of these were located close to known H II regions, and had spectra similar to these H II regions. Of the remaining three, two are classified here as PN and one as a Seyfert 2 galaxy. Coordinates of the three objects are shown in Table 1, along with other catalogue listings for the objects from the SIMBAD database. Observed spectral line strengths and other properties of the objects are given in Table 2. Finder charts for the objects are shown in Figures 1–3. The two PN are the objects IRAS 08418–4847 and IRAS 14132–5839, and the galaxy is IRAS 07245–3548. IRAS 08418–4847 is present in the 'pospn' file of the Strasbourg–ESO Catalogue of Galactic Planetary Nebulae, and is given the object type 'PN?' in the SIMBAD database.

3 The Planetary Nebulae

Each of the objects presented here displays easily resolved emission lines, and no detectable continuum. Spectra of the two PN are shown in Figures 4 and 5. The identified lines are Hβ, along with the 5007 and 4959 Å [O III] 'nebulium' lines labelled as N1 and N2 respectively. In both objects the [O III] lines are significantly stronger than the Hβ line. The objects are spatially unresolved as determined from their intensity profiles along the spectrograph slit. Upper limits on their angular sizes are given in Table 2.

PN are not the only objects that satisfy these properties. Other objects that may display emission-line spectra such as these are novae, compact emission-line galaxies, H II regions, and emission-line stars.

 1323-3580/99/020134$05.00

Table 1. Coordinates and other catalogue designations for the three objects

IRAS	α J2000	δ J2000	l	b	Other designations
07245–3548	07 26 26·3	−35 54 24	248·76	−9·03	PMN J0726–3554
08418–4847	08 43 29·1	−48 54 50	267·37	−3·95	PMN J0843–4854a, PK 267–03, Wray 16–28, PN Sa 3–7
14132–5839	14 16 51·8	−58 53 11	313·78	+2·17	PMN J1416–5853

Table 2. Properties of the objects

Observed optical spectral line fluxes, IRAS and PMN fluxes, ratio of [O III] lines to Hβ, extinction coefficient C, excitation class p, radial velocity v_{rad}, and observed angular diameters

Flux or nebular property	07245–3548	08418–4847	14132–5839
3727 Å [O II] (10^{-14} erg cm^{-2} s^{-1})	8·2	—	—
4861 Å Hβ (10^{-14} erg cm^{-2} s^{-1})	1·4	2·8	1·0
4959 Å [O III] (10^{-14} erg cm^{-2} s^{-1})	7·5	14	3·2
5007 Å [O III] (10^{-14} erg cm^{-2} s^{-1})	22	46	9·8
IRAS 12 μm (Jy)	0·3	0·37	0·3
IRAS 25 μm (Jy)	0·87	3·6	3·4
IRAS 60 μm (Jy)	1·54	4·1	1·9
IRAS 100 μm (Jy)	3·03	24	39
PMN 5 GHz (mJy)	109±13	96±10	34±8
$\frac{(F4959+5007)}{F(H\beta)}$	21	21	13
C	—	3·04	2·98
p	—	≥4	3
v_{rad} (km s^{-1})	8730±66	132±25	−144±15
Diameter ($''$)	≤1·5	≤2·8	≤2·5

Extragalactic objects are easily distinguishable by their larger redshifts, while galactic objects have smaller redshifts. The redshifts of IRAS 08418–4847 and 14132–5839 (Table 2) are typical of galactic objects. While it is not possible to completely rule out all of the other above-mentioned object types, objects with the properties of IRAS 08418–4847 and 14132–5839 are regarded as being PN by the majority of authors (for example Cuisinier, Terzan & Acker 1993). Compact H II regions are generally brighter than PN, and may usually be excluded by the presence of a continuum (Morgan & Good 1992). The six emission-line objects observed in this survey that were classed as H II regions all had some evidence of extended structure on the DSS images.

The level of excitation may be inferred from the ratio of the [O III] lines to Hβ. This ratio is higher on average for PN than for H II regions, since the central stars of PN generally have higher temperatures than in H II regions. The two PN (and the galaxy) of this survey all have a higher (N1+N2)/Hβ ratio than any of the six observed HII regions. In addition, both PN lie well inside the infrared colour box described by Pottasch et al. (1988), far away from the region where H II regions are usually found.

The excitation class p is calculated for each of the PN as described by Gurzadyan (1997), and shown in Table 2. The lower classes are based on the (N1+N2)/Hβ ratio, up to $p = 4$ for (N1+N2)/H$\beta > 15$. For classes higher than $p = 4$, the 4686 Å line of He II is used, however, this line was not observed in either of the objects.

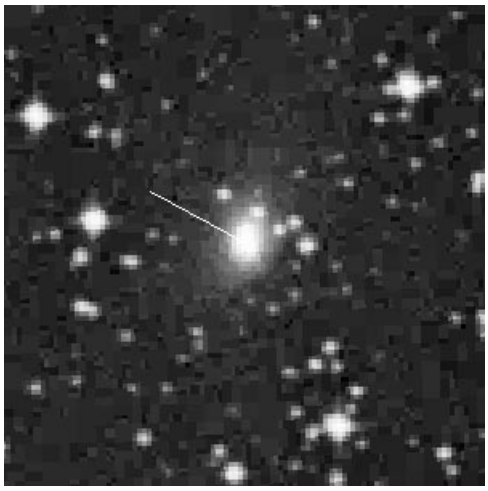

Figure 1—Finder chart for IRAS 07245–3548.

Milne & Aller (1975) derived a method for estimating the distances to planetary nebulae using the 5 GHz radio flux. The method is based on average values, over a large number of planetary nebulae, for the parameters $y = 0{\cdot}11$, $\varepsilon = 0{\cdot}6$, $T_e = 10\,000$ K, $x'' = 0{\cdot}5$ and $M = 0{\cdot}16$ M$_\odot$. Here y is the number abundance ratio of helium to hydrogen, x'' is the fraction of He III to He I atoms, and M is the nebular mass. The *filling factor* ε measures the degree of divergence of the nebula from homogeneity. The distance is

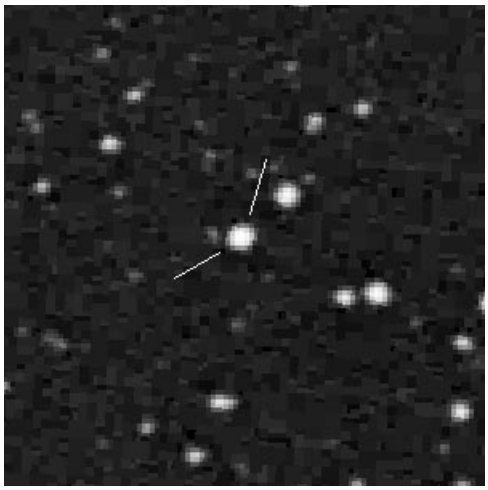

Figure 2—Finder chart for IRAS 08418–4847.

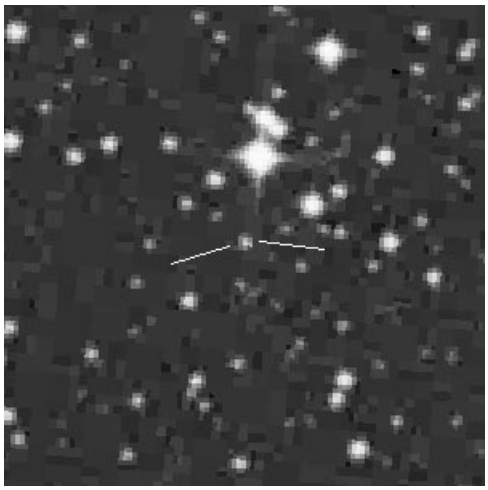

Figure 3—Finder chart for IRAS 14132–5839.

$$D = 6180\theta^{-3/5}F_{5\mathrm{GHz}}^{-1/5}\,, \qquad (1)$$

where D is given in parsecs, θ is the angular diameter of the nebula in arcseconds, and F is given in Janskys. Using angular sizes from Table 2, this method gives a lower limit of $D \geq 5300$ pc for IRAS 08418–4847 and $D \geq 7000$ pc for IRAS 14132–5839. Milne & Aller (1975) also gave a method for estimating the expected flux in Hβ from the 5 GHz radio flux. The expected Hβ flux is given by

$$\frac{10^{-26}F_{5\mathrm{GHz}}}{F(\mathrm{H}\beta)} = 3{\cdot}05\times10^{-18}\,t^{0{\cdot}4}\ln(9900\,t^{\frac{3}{2}}) + \left\{1+(1-x'')y+3{\cdot}7x''y\right\}, \qquad (2)$$

with $t = T_e/10^4$ K, $F(\mathrm{H}\beta)$ in erg cm^{-2} s^{-1}, and $F_{5\mathrm{GHz}}$ in Jy, as before. Using the average values for T_e, x'', and y quoted previously, this method gives a predicted Hβ flux of $3{\cdot}1\times10^{-11}$ erg cm^{-2} s^{-1} for IRAS 08418–4847 and $9{\cdot}6\times10^{-12}$ erg cm^{-2} s^{-1} for IRAS 14132–5839. Comparing the predicted and observed fluxes in Hβ gives a measure of the interstellar extinction between the source and the Earth. The extinction coefficient C, calculated as

$$C = \log_{10}\left(\frac{F(\mathrm{H}_\beta)\ \text{predicted}}{F(\mathrm{H}_\beta)\ \text{observed}}\right), \qquad (3)$$

is shown in Table 2 for the two objects.

A second method of calculating distances to PN is quoted by several authors, for example Pottasch (1984). This method uses the Hβ flux alone and applies to PN with densities higher than 4×10^2

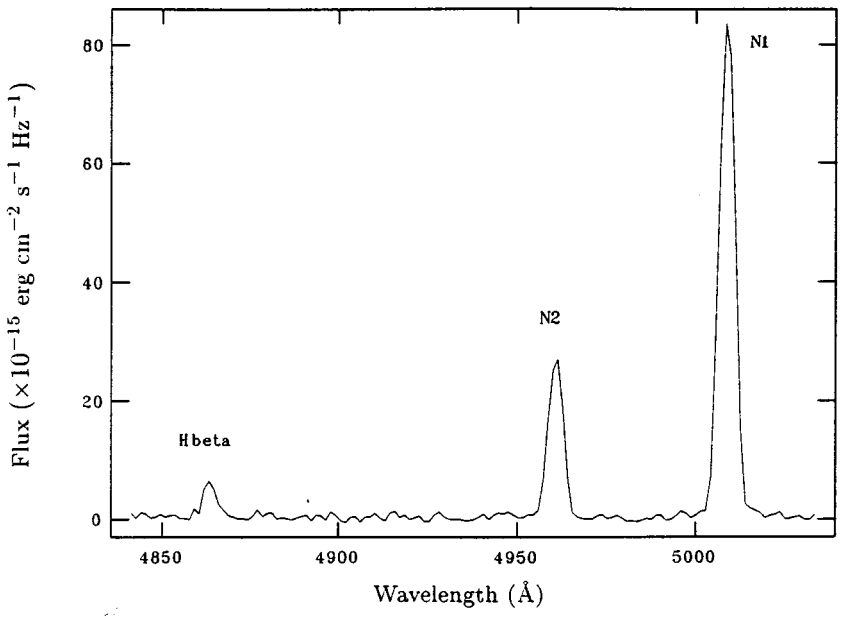

Figure 4—[O III] and Hβ lines IRAS 08418–4847.

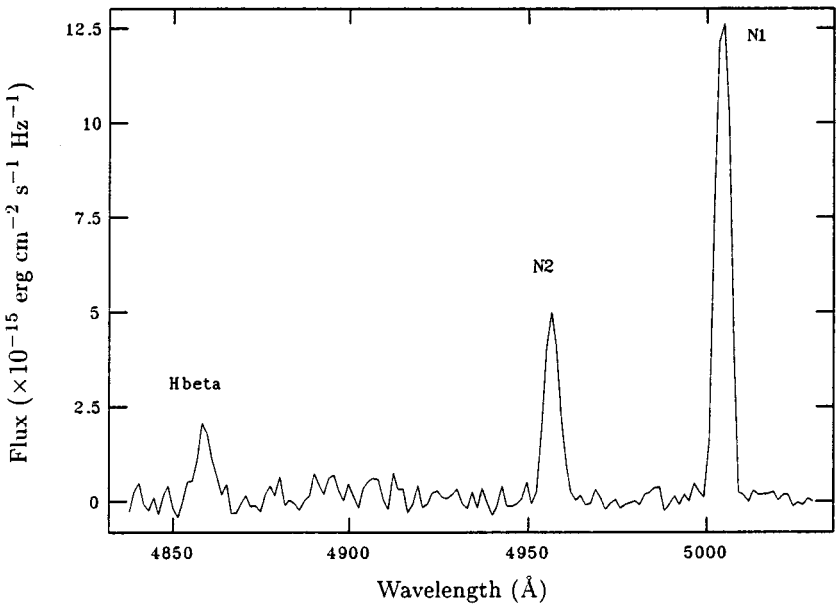

Figure 5—[O III] and Hβ lines in IRAS 14132–5839.

particles cm^{-3}. From an examination of known PN data, it is apparent that for PN of high density, assuming a constant average mass (such as the $M = 0{\cdot}16$ M$_\odot$ used above) gives a poor approximation. A better approximation is to take the mass as $M = 10^2$ M$_\odot$ cm$^{-3}\, n_e^{-1}$, which has the convenient effect of removing the dependence on angular size seen in equation (1). Using this approximation, the distance is given by

$$D = 3\,\{F(\mathrm{H}\beta)\}^{-1/2}\,, \qquad (4)$$

with D in kiloparsecs and $F(\mathrm{H}\beta)$ in 10^{-11} erg cm^{-2} s^{-1}. The Hβ value to be used is that corrected for interstellar extinction, and thus the values estimated from the radio flux are used, giving distances of 1700 pc and 3100 pc to IRAS 08418–4847 and 14132–5839 respectively.

Clearly the two methods used give significantly different distances. This may be explained in terms of the inherently low accuracy of these statistical distance methods and the unknown density of the nebulae. The densities may be low, and thus equation (4) would not apply. Alternatively, the density may be high, and thus the constant mass method of equation (1) gives a poor approximation.

A recent treatment of distances to PN has been given by Schneider & Buckley (1996). Their method uses an empirically determined relationship between surface brightness and radius, in the form of a second-degree polynomial fit to a selection of PN. The method is thus more reliable, and able to cope with a larger range of physical properties of PN. Specifically, the method gives better results for PN of both high and low density and surface brightness.

Using this method, the radius–surface brightness relationship is

$$\log\, r = a\,(\log\, I_\nu)^2 + b\,(\log\, I_\nu) + c\,. \qquad (5)$$

Here r is the nebular radius in pc, $I_\nu = F_{5\mathrm{GHz}}/(\pi\theta^2)$ is the surface brightness in mJy arcsec^{-2}, and $a = -0{\cdot}0261$, $b = -0{\cdot}299$, and $c = -1{\cdot}116$ are empirically determined constants. The distance D in kpc is then given by

$$\log\, D = \log\, r - \log\, \theta + \log\, 206{\cdot}265\,, \qquad (6)$$

with θ measured in arcsec. This method gives a distance of $D \geq 3700$ pc for IRAS 08418–4847 and $D \geq 5300$ pc for IRAS 14132–5839. The nebular radii estimated using equation (5) are $r \leq 0{\cdot}050$ pc for IRAS 08418–4847 and $r \leq 0{\cdot}065$ pc for IRAS 14132–5839. The distance figures given by this recent method are seen to be between those given by the earlier two methods.

4 The Seyfert Galaxy

The spectrum of this object is shown in Figure 6, which is the average of four separate CCD exposures. The radial velocity of 8730 km s^{-1} and clearly defined emission lines from a small area $\leq 1{\cdot}5$ arcsec in diameter are typical of an active galactic nucleus (AGN). The emission-line source is at the centre of a larger optical source of size $\sim 20'' \times 30''$, and a still larger radio source of size $\sim 1{\cdot}5'$ in diameter. A radio image of the object is shown in Figure 7, taken from the VLA NVSS at 1·4 GHz. This image is approximately $15' \times 15'$ in size.

Distance is estimated at 120 Mpc using a Hubble constant of 75 km s^{-1} Mpc^{-1}. Linewidths are ∼500 km s^{-1}, and the 5 GHz power output, calculated from the PMN flux and a distance of 120 Mpc, is 2×10^{23} W Hz^{-1}. Classification of this object as a Seyfert 2 galaxy is based on its known properties and

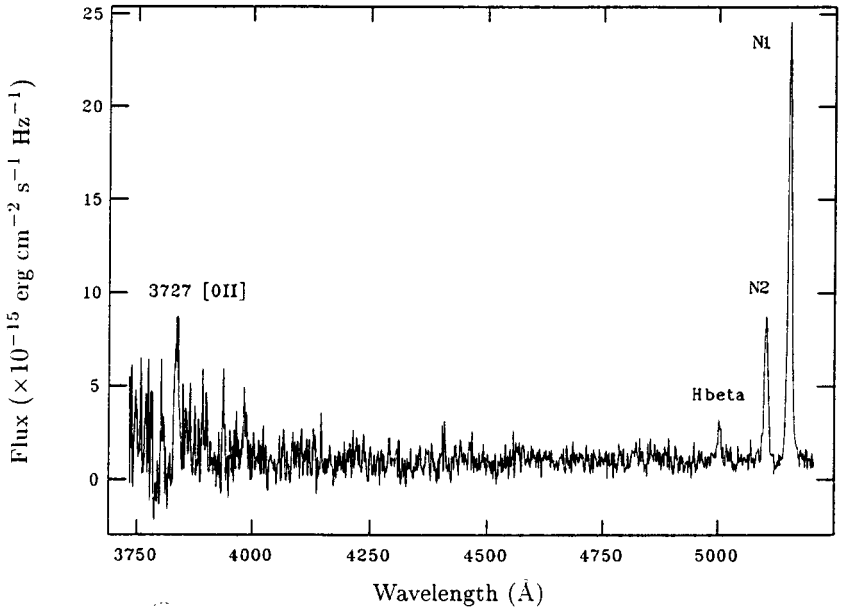

Figure 6—Spectrum of IRAS 07245–3548.

the properties of the various AGN classes discussed by Woltjer (1990).

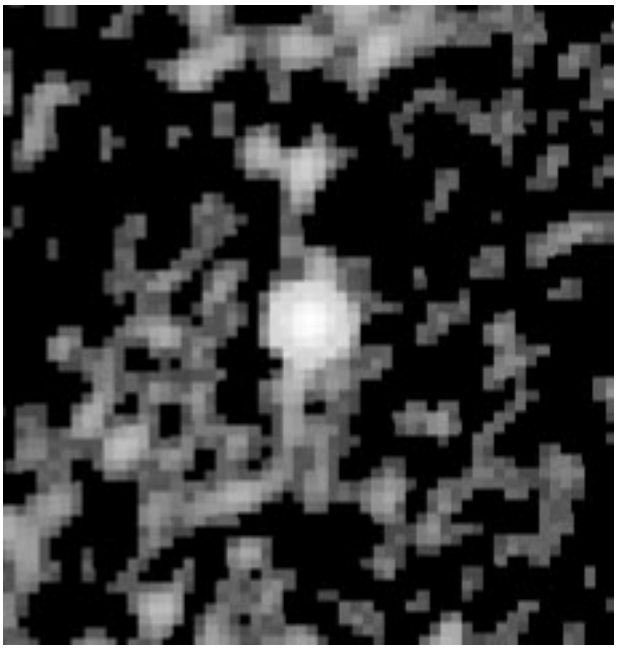

Figure 7—A 1·4 GHz radio image of IRAS 07245–3548.

The presence of the λ3727 [O II] line is typical of PN and of many AGN types, including Seyfert galaxies. However, in PN, the excitation is produced by a central star, with an approximately blackbody continuum, in a relatively narrow range of wavelengths. The power-law spectra of AGN are broader, and allow a wider range of excitation states to be seen. In this object, the λ3727 [O II] and the [O III] lines are all much stronger than Hβ, a feature not typically seen in nebulae excited by starlight. Woltjer (1990) quoted typical values for the flux ratios λ5007 [O III]/Hβ and 3727 [O II]/Hβ for Seyfert 2 galaxies as 13 and 2 respectively. For IRAS 07245–3548 these ratios are 16 and 5 respectively, which may suggest a broader than average range of ionisation states.

5 Conclusions

Low-resolution spectra have been presented for one previously known 'possible PN' and for two completely new objects. The SIMBAD database contains no nonstellar objects within 15′ and 7′ radii of IRAS 07245–3548 and 14132–5839 respectively, apart from the IRAS and PMN entries. IRAS 07245–3548 is thus not in any catalogue of known galaxies included in SIMBAD, active or ordinary.

Acknowledgments

We would like to thank Mount Stromlo and Siding Spring Observatories for providing observing time on the 74 in Telescope, and N. Penney for her assistance with the observations.

References

Cuisinier, F., Terzan, A., & Acker, A. 1993, A&A, 277, 203
Gurzadyan, G. A. 1997, The Physics and Dynamics of Planetary Nebulae (Berlin: Springer)
Milne, D. K., & Aller, L. H. 1975, A&A, 38, 183
Morgan, D. H., & Good, A. R. 1992, A&AS, 92, 571
Pottasch, S. R. 1984, Planetary Nebulae—A Study of Late Stages of Stellar Evolution (Dordrecht: Reidel)
Pottasch, S. R., Bignell, C., Olling, R., & Zijlastra, A. A. 1988, A&A, 205, 248
Schneider, S. E., & Buckley, D. 1996, ApJ, 459, 606
Van de Steene, G. C., & Pottasch, S. R. 1993, A&A, 274, 895
Van de Steene, G. C., Sahu, K. C., & Pottasch, S. R. 1996, A&AS, 120, 111
Woltjer, L. 1990, in Active Galactic Nuclei, ed. R. D. Blandford et al. (Berlin: Springer)